Personal Identification Using Periocular Skin Texture

Philip E. Miller
Clemson University
Clemson, SC 29634, USA
pemille@clemson.edu

Allen W. Rawls
Clemson University
Clemson, SC 29634, USA
arawls@clemson.edu

Shrinivas J. Pundlik
Clemson University
Clemson, SC 29634, USA
spundli@clemson.edu

Damon L. Woodard
Clemson University
Clemson, SC 29634, USA
woodard@clemson.edu

ABSTRACT

In this paper, we propose the use of periocular skin texture as a biometric modality. Salient skin texture features are extracted and represented using Local Binary Patterns (LBPs). Matching is performed using CityBlock distance as a measure of similarity. We investigate the use of each periocular region separately in addition to their use in conjunction. Verification and identification experiments involving over 400 subjects were performed using a datasets constructed from the FRGC and FERET datasets. Reported recognition rates of nearly 90%, demonstrate the effectiveness of this novel technique.

Keywords

biometrics, periocular region features, texture analysis, local binary patterns

1. INTRODUCTION

In recent years, researchers have utilized a number of biometric modalities to accurately identify individuals. Two of the more commonly used modalities are facial features and iris texture. Although both modalities have achieved high recognition rates, each requires high quality input images and are hindered by the presence of non-ideal images. Such images are either not suitable for identification purposes, or would result in less accurate recognition. As a result, researchers are looking for ways to make use of the images despite their low quality, where localized biometric discriminative features would aid in the task of recognition. One such area is the periocular region of the face, which is a small region surrounding the eye as shown in Figure 1. It is known to be a feature-rich region and contains a significant amount of discriminating information [11]. The periocular features can be classified into level-one and level-two features. Examples of level-one features include the upper/lower eye folds, the upper/lower eyelid, wrinkles, and moles. Level-two features are more detailed and include skin textures, pores, hair follicles, skin tags, and other fine dermatological features. This research explores the potential for robust level-two feature extraction in the periocular region for identification when the full face is partially occluded or the image quality is insufficient for iris texture extraction. In this work we use only the periocular region images captured within the visible spectrum.

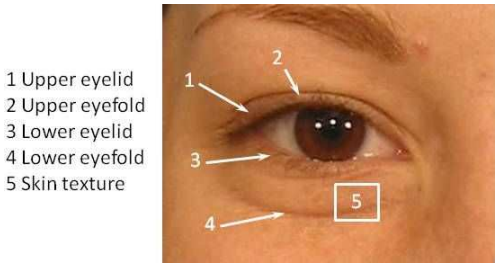

Figure 1: Features present in the human periocular region.

2. LBP-BASED PERIOCULAR REGION FEATURES

For the extraction and analysis of periocular features, Local Binary Patterns are the chosen method of extrapolation. Local Binary Patterns (LBP), as first introduced by Ojala et al. in [6], quantify intensity patterns or textures of local pixel neighborhood patches, which are pre-divided sections of a given image. LBPs are useful for identifying spots, line ends, edges, corners, and other distinct texture patterns. They are also practical for biometric applications such as face recognition [1, 3, 16, 17], face detection [2], facial expression recognition [5, 12], gender classification [4, 13], iris recognition [14], and palm print identification [15]. For these reasons, LBP was chosen as the best method to explore the periocular region. The textures quantified by LBP in an image patch are encoded into a histogram. The following is a high level description of how the LBP histogram is computed from an image. For a more thorough description of the method see [7].

The texture T of a local neighborhood is computed from $P+1$ pixels ($P > 0$) on a circle of radius R ($R > 0$).

$$T = t(g_c, g_0, \ldots, g_{P-1}), \quad (1)$$

describes a texture neighborhood, where g_c is the intensity at the center pixel, and g_p, $p = 0, \ldots, P-1$, is the intensity of the p^{th} pixel. Intensity values of locations along the circle that do not fall in the center of a pixel in the image are computed using interpolation.

SAC'10 March 22-26, 2010, Sierre, Switzerland.

Two modifications can be made to T in (1) to achieve illumination invariance. The pixels of T can be represented as a joint distribution of the difference between intensities of the P pixels and the center pixel. The intensity of the center pixel is independent of the intensity differences of the other pixels. This leads to

$$T \approx t(g_0 - g_c, \ldots, g_{P-1} - g_c). \quad (2)$$

Scale invariance can be added to (2) by using the signs of the differences instead of the actual intensity differences as in,

$$T \approx t(s(g_0 - g_c), \ldots, s(g_{P-1} - g_c)), \quad (3)$$

where

$$s((g_p - g_c)) = \begin{cases} 1 & if g_p - g_c \geq 0 \\ 0 & if g_p - g_c < 0. \end{cases}$$

To compute the LBP operator for each pixel neighborhood, the elements in (3) are given a binomial weight as in

$$LBP_{P,R}(x_c, y_c) = \sum_{p=0}^{P-1} s(g_p - g_c) 2^P. \quad (4)$$

The $LBP_{P,R}$ operator gives 2^P output values. These are the 2^P binary patterns found in the P pixel neighborhood. Certain fundamental patterns are defined as "uniform" in a 3×3 neighborhood. A uniformity measure $U(pattern)$ is defined and corresponds to the number of 0/1 bitwise or sign changes in the pattern. For this paper, uniform patterns have a U value of 2. The uniform LBP operator, $LBP^{u2}_{P,R}$, is defined as

$$LBP^{u2}_{P,R} = \begin{cases} \sum_{p=0}^{P-1} s(g_p - g_c), & if U(LBP_{P,R}) \leq 2 \\ P + 1, & otherwise, \end{cases}$$

where

$$\begin{aligned} U(LBP_{P,R}) &= |s(g_{P-1} - g_c) - s(g_0 - g_c)| \\ &+ \sum_{p=1}^{P+1} |s(g_p - g_c) - s(g_{p-1} - g_c)|. \end{aligned}$$

The occurrences of each LBP value are stored in a histogram. Each histogram has $P * (P - 1) + 3$ bins. There are P uniform patterns that contain only a single bit change. There are $P - 1$ uniform patterns for each of the P bit changes and an addition bit change. The 3 remaining bins store the 2 uniform patterns where $U(pattern) = 0$ and all non-uniform patterns. An eight neighbor histogram of 3×3 has 59 bins.

3. PERIOCULAR REGION DATA

To our knowledge, a publicly available dataset of periocular region images does not exist. For this reason, two commonly used facial recognition datasets were used to construct a dataset for experimentation. The periocular region images created for these experiments come from a subset of the frontal face images in the Facial Recognition Grand Challenge (FRGC) database [8] and the Facial Recognition Technology (FERET) database [9], [10]. The experimental subset contains only neutral expression face images. Subjects that wear glasses were omitted as well as subjects without multiple images. The FRGC database was collected at the University of Notre Dame over a two year period and consists mainly of subjects between the ages of 18 and 22. The purpose of the FRGC was to advance face recognition technology to support existing efforts of the U.S. Government. The FERET database is a collection of biometric data sponsored by the Department of Defense for the purpose of assisting security, intelligence, and law enforcement. The images were intended to be used in evaluating the effect of aging of subjects and changes in facial expression.

Figure 2: (LEFT TO RIGHT:) **A face image with cropping regions overlain, cropped right periocular region image, and cropped left periocular region image.**

Unlike the FRGC database, most of the subjects in the FERET database contain only one neutral expression image. This allows the FRGC experiments to be done with significantly more images. Using provided eye center coordinates, two separate periocular region images are extracted for each eye from the original facial image with bounds calculated by a ratio computed by the distance between the eyes. These extracted images, as compared to the original facial image, are shown in Figure 2, where the eye insets are samples of the data extracted from the full facial image.

All periocular region images can be scaled to uniform sizes, because they were extracted using the same ratio. The periocular region images are 100×160 pixels. Each image goes through histogram normalization and is then segmented into 24 different 25×25 pixel blocks beginning at the origin. Using LBP, each image can be represented as a vector of LBP histogram bins for each patch (a total of 1,416 elements). To eliminate the effect of textures in the iris and the surrounding sclera area, an elliptical mask of neutral color is placed over in the middle of the periocular region image. The steps for feature extraction are shown in Figure 3, where (a) normalized periocular region image, (b) image separated into 25×25 pixel blocks, (c) LBP encoded image, (d) masked normalized image, and (e) the LBP histogram for a block of pixels.

Two sets of experiments evaluate the performance of the LBP operator on periocular images from the selected databases. Let these be called **FRGC** and **FERET**. In order to narrow the search for identifying features in the periocular region, sub-experiments divide the images into three sets, focusing on each eye individually and then both eyes together. The sub-experiments using only right eyes are referred to as **FRGC_R** and **FERET_R**; left eyes are **FRGC_L** and **FERET_L**; both eyes are **FRGC_B** and **FERET_B**. Each of these sets consist of a single probe and two gallery images per subject. All probe images were captured after their respective gallery images. There are 410 subjects for a total of 1,230 images used in each FRGC experiment. There are 54 subjects for a total of 162 images used in the FERET experiment.

4. RESULTS AND DISCUSSION

Performance of the LBP operator on the periocular region images for the identification experiments is determined by computing CityBlock distances between the probe image and each of the gallery images. CityBlock is given by the following:

$$D_{CB}(\mathbf{u}, \mathbf{v}) = \sum_{i=1}^{N} |\mathbf{u}_i - \mathbf{v}_i|, \quad (5)$$

where $\mathbf{u}$ and $\mathbf{v}$ are the N dimensional LBP feature vector representations of two images. The relationship between these distances are presented using several fundamental biometric graphs, detailed

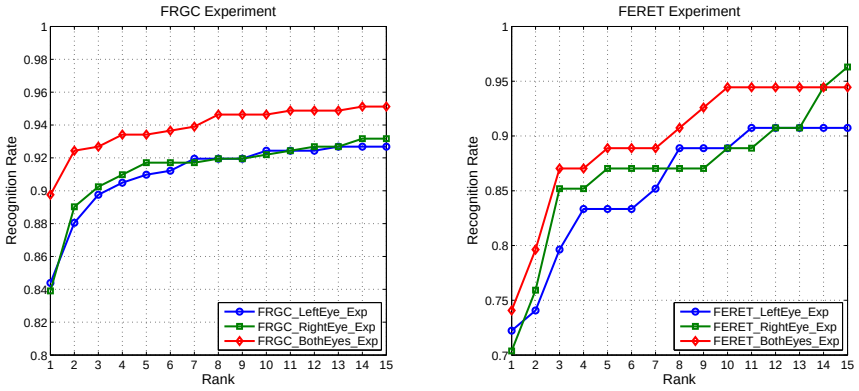

(a) (b)

Figure 4: Cumulative match characteristics (CMC) curves for (a) FRGC, and (b) FERET experiments.

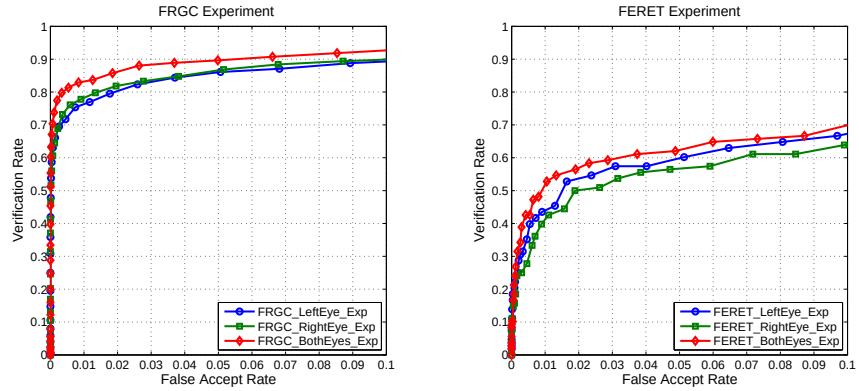

(a) (b)

Figure 5: Receiver operating characteristics (ROC) curves for (a) FRGC, and (b)FERET experiments.

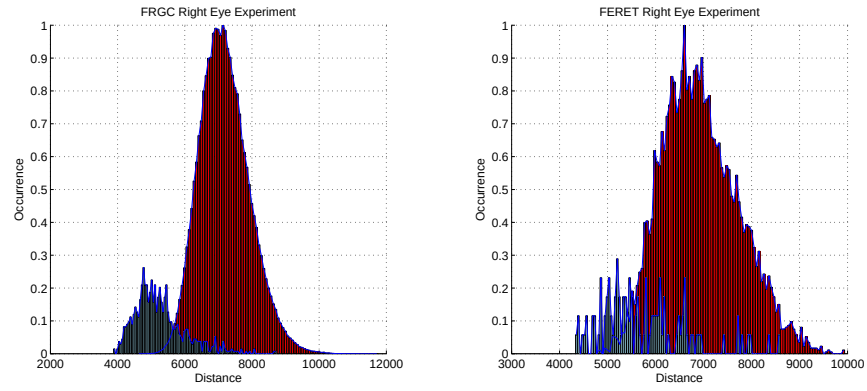

(a) (b)

Figure 6: Histograms of class separability for two sub-experiments, (a) FRGC_R, and (b)FERET_R.

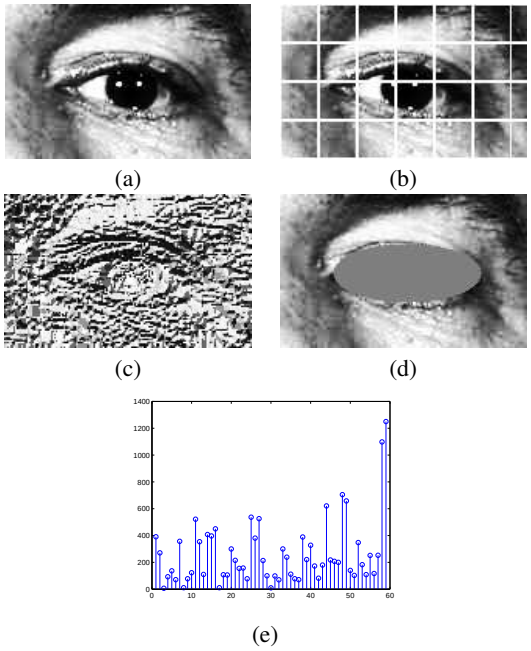

Figure 3: Sample images for: (a) normalized periocular region image, (b) image separated into 25×25 pixel blocks, (c) LBP encoded image, (d) masked normalized image, and (e) the LBP histogram for a block of pixels.

below.

A Cumulative Match Curve (CMC) graph gives a visual representation of performance of an identification system. A given recognition rate (plotted on the y-axis) at Rank x (plotted on the x-axis) corresponds to the percent of times the correct match for a subject is made in the top x closest images. Rank 1 recognition rates show the effectiveness of the system at choosing the best match for a subject. Figure 4 shows the CMC graphs computed for the two experiments. Table 1 presents the Rank 1 recognition rates of all experiments. **FERET** has a lower Rank 1 recognition than **FRGC**. This is attributed to lesser image quality of images in the FERET dataset. However, the results for both **FERET** and **FRGC** are significant. For both experiments, the left eye performs better than the right eye, while identification using both eyes combined is observed as the best method. Distances for experiments using both eyes were calculated by summing the distances of the left and right eye experiments.

In addition to identification experiments, verification experiments are performed using the same datasets and visualized using Receiver Operating Characteristic (ROC) Curves. Genuine match rates, also known as the verification rate or VR, and impostor match rates, also known as false accept rate or FAR, are computed and plotted to display the ROC curve, shown in Figure 5. The statistical measure that best communicates the quality of the ROC curve is the Equal Error Rate or EER. An EER is the rate at which the false accept rate and false reject rate, FRR are equal ($FRR = 1 - VR$). A lower EER corresponds to a more accurate verification system. The EER rates for each of the six sub-experiments are shown in Table 1. The genuine match score distribution and the impostor distributions are plotted in Figure 6. The separation of the distributions is much better in the experiments involving FRGC data (a) as compared to those using the FERET data (b). This is partly the result of the higher resolution of the FRGC images compared to the FERET images. In addition, significantly less images are used in the FERET experiments which could affect overall recognition rates.

	Rank 1 recognition rate	EER
FRGC_L	84.39%	0.1019
FRGC_R	83.90%	0.1098
FRGC_B	89.76%	0.0853
FERET_L	72.22%	0.2179
FERET_R	70.37%	0.2259
FERET_B	74.07%	0.2320

Table 1: Summary of observations from the CMC and ROC curves

5. CONCLUSIONS AND FUTURE WORK

This paper demonstrates that periocular skin texture computed by LBP shows promise as a novel biometric for establishing identity. The experiments presented in this paper measure the performance of the new biometric on the problem of identification and verification on periocular region image data collected from over 400 individuals. Furthermore, the separability of classes strongly suggest that the skin texture, eye folds, and contours of the periocular region hold discriminating ability and can adequately verify a person's identity.

Future work in this area would include the fusion of periocular region based identification with iris texture based systems. Periocular features could possibly be used to address situations in which the iris is occluded, dilated, or out of focus within the image. Our future work would also include the use of other texture feature extraction/representation techniques, more sophisticated matching techniques, and an investigation into the effects of facial expression/less controlled imaging conditions on periocular based recognition performance.

6. REFERENCES

[1] G. Heusch, Y. Rodriguez, and S. Marcel. Local binary patterns as an image preprocessing for face authentication. *Proc. of International Conference on Automatic Face and Gesture Recognition*, pages 9–14, 2006.

[2] H. Jin, Q. Liu, H. Lu, and X. Tong. Face detection using improved lbp under bayesian framework. *Third International Conference on Image and Graphics (ICIG)*, pages 306–309, 2004.

[3] S. Z. Li, R. Chu, M. Ao, L. Zhang, and R. He. Highly accurate and fast face recognition using near infrared images. *Proc. Advances in Biometrics, International Conference, Lecture Notes in Computer Science 3832, Springer*, pages 151–158, 2006.

[4] H. Lian and B. liang Lu. Multi-view gender classification using local binary patterns and support vector machines, tsallis entropies and global appearance features. *Proc. 3rd International Symposium on Neural Networks (ISNN)*, pages 202–209, 2006.

[5] S. Liao, W. Fan, A. Chung, and D. Yeung. Facial expression recognition using advanced local binary patterns, tsallis entropies and global appearance features. *Proc. of the IEEE*

International Conference on Image Processing (ICIP), pages 665–668, 2006.

[6] T. Ojala, M. Pietikäinen, and D. Harwood. A comparative study of texture measures with classification based on feature distribution. *Pattern Recognition*, 29(1):51–59, 1996.

[7] T. Ojala, M. Pietikäinen, and T. Mäenpää. Multiresolution gray-scale and rotation invariant texture classification with local binary patterns. *IEEE Transactions on Pattern Analysis and Machine Intelligence (PAMI)*, 24(7):971–987, 2002.

[8] P. J. Phillips, P. J. Flynn, T. Scruggs, K. W. Bowyer, J. Chang, K. Hoffman, J. Marques, J. Min, and W. Worek. Overview of face recognition grand challenge. *IEEE Conference on Computer Vision and Pattern Recognition*, 2005.

[9] P. J. Phillips, H. Moon, S. A. Rizvi, and P. J. Rauss. The feret evaluation methodology for face recognition algorithms. *IEEE Trans. Pattern Analysis and Machine Intelligence*, 22:1090–1104, 2000.

[10] P. J. Phillips, H. Wechsler, J. Huang, and P. Rauss. The feret database and evaluation procedure for face recognition algorithms. *Image and Vision Computing*, 16(5):295–306, 1998.

[11] M. Savvides, R. Abiantun, J. Heo, C. Xie, and B. K. Vijayakumar. Partial and holistic face recognition on frgc ii using support vector machines. *Proc. of IEEE Computer Vision Workshop (CVPW)*, page 48, 2006.

[12] C. Shan, S. Gong, and McOwan. Robust facial expression recognition using local binary patterns. *Proc. of the IEEE International Conference on Image Processing (ICIP)*, pages 370–373, 2005.

[13] N. Sun, W. Zheng, C. Sun, C. Zou, and L. Zhao. Gender classification based on boosting local binary patterns. *International Symposium on Neural Networks (ISNN)*, pages 194–201, 2006.

[14] Z. Sun, T. Tan, and X. Qiu. Graph matching iris image blocks with local binary pattern. *Proc. Advances in Biometrics, International Conference (ICB), Lecture Notes in Computer Science 3832, Springer*, pages 366–373, 2006.

[15] X. Wang, H. Gong, H. Zhang, B. Li, and Z. Zhuang. Palmprint identification using boosting local binary pattern. *Proc. 18th International Conference on Pattern Recognition (ICPR)*, 2006.

[16] H. Zhang and D. Zhao. Spatial histogram features for face detection in color images. *Advances in Multimedia Information Processing - PCM 2004: 5th Pacific Rim Conference on Multimedia*, pages 377–384, 2004.

[17] W. Zhang, S. Shan, H. Zhang, W. Gao, and X. Chen. Multi-resolution histograms of local variation patterns (mhlvp) for robust face recognition. *Proc. Audio- and Video-Based Biometric Person Authentication: 5th International Conference (AVBPA), Lecture Notes in Computer Science 3546, Springer*, pages 937–944, 2005.

PHILIP E. MILLER - received the B.S. degree in Computer Science from Clemson University in 2008. He is currently a Ph.D. student in the School of Computing at Clemson University. His research interest include biometrics and image processing.

ALLEN W. RAWLS - is a Ph.D. student in the School of Computing at Clemson University. He received his B.S. and M.S. degrees in Computer Science from the University of North Carolina Wilmington in 2006 and 2008 respectively. His research interest include biometrics, image processing, and location-based mobile computing.

SHRINIVAS J. PUNDLIK - received the B.E. degree in electronics engineering from Pune University, India, in 2002, and the M.S. and Ph.D. degrees in electrical engineering from Clemson University in 2005 and 2009 respectively. He is currently working as a research associate in Clemson University's School of Computing. His research interests include image and motion segmentation, pattern recognition, and biometrics.

DAMON L. WOODARD - received his Ph.D. in Computer Science and Engineering from the University of Notre Dame, his M.E. in Computer Science and Engineering from Penn State University, and his B.S. in Computer Science and Computer Information Systems from Tulane University in 1997, 1999, and 2004 respectively. He is currently an Assistant Professor at Clemson University in the School of Computing where he has established the Biometrics and Pattern Recognition Lab (BPRL). His research interests are biometrics, pattern recognition, and machine learning. Prior to joining Clemson University in 2006, Dr. Woodard was a Director of Central Intelligence postdoctoral fellow. His postdoctoral research focused on the development of advanced iris recognition systems using high resolution sensors.